Nanoscale

PAPER

View Article Online
View Journal | View Issue

Cite this: *Nanoscale*, 2015, **7**, 4250

Effect of surface roughness on substrate-tuned gold nanoparticle gap plasmon resonances

Chatdanai Lumdee,[a] Binfeng Yun[b] and Pieter G. Kik*[a,c]

Received 7th October 2014,
Accepted 2nd February 2015

DOI: 10.1039/c4nr05893c

www.rsc.org/nanoscale

The effect of nanoscale surface roughness on the gap plasmon resonance of gold nanoparticles on thermally evaporated gold films is investigated experimentally and numerically. Single-particle scattering spectra obtained from 80 nm diameter gold particles on a gold film show significant particle-to-particle variation of the peak scattering wavelength of ±28 nm. The experimental results are compared with numerical simulations of gold nanoparticles positioned on representative rough gold surfaces, modeled based on atomic force microscopy measurements. The predicted spectral variation and average resonance wavelength show good agreement with the measured data. The study shows that nanometer scale surface roughness can significantly affect the performance of gap plasmon-based devices.

Introduction

Substrate-tuned metal nanoparticle systems are promising for use in plasmon-enhanced biochemical sensing applications due to their ability to provide large electric field enhancement at controlled resonance wavelengths.[1–4] These structures are typically defined by depositing noble metal particles onto a metal-coated substrate, where near-field interaction between the plasmon resonant particle and free charges in the substrate dramatically changes the optical response of the particle. Unlike plasmonic structures defined by electron beam lithography or other top-down approaches, such film-coupled nanoparticle systems are easy to fabricate, are compatible with single-crystalline chemically synthesized metal nanoparticles, and produce a well-defined hot-spot at the gap between the nanoparticle and the substrate (gap plasmon). Recent studies have shown that combining film-coupled nanoparticle structures with an inorganic spacer can improve their stability under laser irradiation while maintaining large field enhancement factors, making them great candidates for reliable optical sensors.[5,6] A common method for preparing such systems involves particle deposition from colloidal suspensions onto thermally evaporated metal films. On such samples, variations in resonance frequency are routinely observed despite the use of solutions with a narrow particle size distribution. These spectral variations may be related to several factors, including nanoparticle size/shape variations, variations in local dielectric environment, and the presence of film surface roughness. While the effect of particle size, shape variation, and local dielectric function on the particle resonances has been widely studied (see for example ref. 7–10), the effect of surface roughness has received relatively little attention.[11]

In this article, we investigate the effect of surface roughness on the gap plasmon resonance of gold nanoparticles in a substrate-tuned nanoparticle system. Single-particle scattering spectra of gold nanoparticles on a thermally deposited gold film were measured, revealing significant spectral variations. To understand these observations numerical simulations of representative local nanoscale geometries were carried out and compared with the measured spectra. The results indicate that the experimentally observed spectral variation can be understood in terms of the measured surface roughness, highlighting the importance of the film surface morphology on the reliability of substrate-tuned nanoparticle structures. These effects cannot be readily observed in ensemble measurements, but are expected to play a crucial role in determining the performance of nanoparticle based plasmonic devices.

Results and discussion

Fig. 1(a) shows a darkfield microscopy image of a representative area of the sample, showing sparsely distributed gold nanoparticles on a gold film coated with a 4-methylbenzenethiol (4-MBT) monolayer. Details of our sample preparation method can be found in the Experimental section. The particles exhibit similar scattering color and intensity, with most particles producing a red ring and a weak central green spot as seen in the insets in Fig. 1(a). These features are known to cor-

[a]*CREOL, The College of Optics and Photonics, University of Central Florida, 4000 Central Florida Blvd, Orlando, FL 32816, USA*
[b]*Advanced Photonics Center, School of Electronic Science and Engineering, Southeast University, Nanjing 210096, China*
[c]*Physics Department, University of Central Florida, 4000 Central Florida Blvd, Orlando, FL 32816, USA. E-mail: kik@creol.ucf.edu*

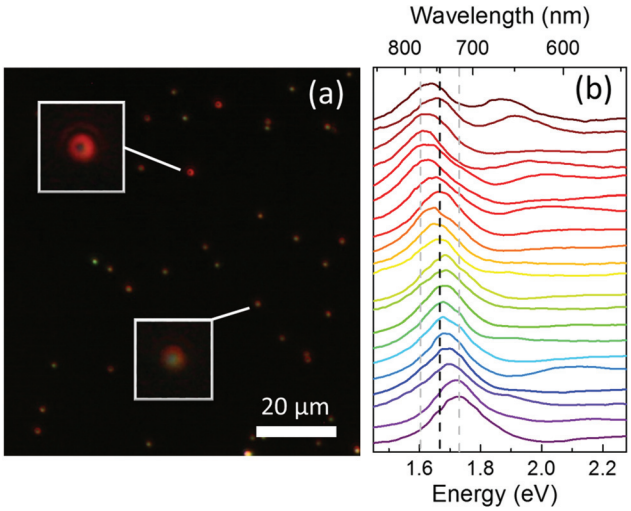

Fig. 1 (a) A darkfield microscopy image of gold nanoparticles on a gold film. The insets show a magnified view of two representative particles. (b) Peak-normalized single particle scattering spectra from randomly selected gold nanoparticles.

respond to scatterers with a low-frequency (red) vertically polarized scattering resonance and a high-frequency (green) predominantly laterally polarized resonance.[6] Fig. 1(b) presents peak-normalized single particle scattering spectra from 21 gold nanoparticles on the gold film. Only particles separated from their nearest neighbor by several μm were selected, but otherwise their selection was made at random. The spectra were approximately sorted by peak scattering energy to facilitate comparison between spectra. The vertical black dashed line indicates the average peak resonance energy of the scattering spectra at 1.67 eV (745 nm). The vertical gray dashed lines represent the statistical variation in peak position spanning two standard deviations on each side ($\pm 2\sigma$ = ±63 meV). Spectral variation of this magnitude could significantly affect the performance and reliability of this substrate-tuned nanoparticle plasmonic system when used *e.g.* as a SERS substrate.

To trace the origin of the observed spectral variations, we first consider the effect of surface roughness on single particle scattering spectra by simulating representative geometries. This is a challenging issue: due to the largely random nature of the surface roughness, each particle is situated in a slightly different local environment. In order to find representative geometries, first the surface morphology was measured using Atomic Force Microscopy (AFM), revealing a root mean square roughness of ~1.2 nm. It was assumed that the liquid-based particle deposition places the particles at local height minima. Possible particle locations were found using a numerical algorithm that extracted the lowest geometrically possible *z*-position of an 80 nm diameter nanosphere at each lateral position of the AFM scan. Each local *z*-minimum from this data set was considered to be a possible particle location after deposition. Fig. 2(a) shows the AFM image of the gold film used in this analysis. Fig. 2(b) shows a zoomed-in perspective of the sample surface at a randomly selected local minimum, with

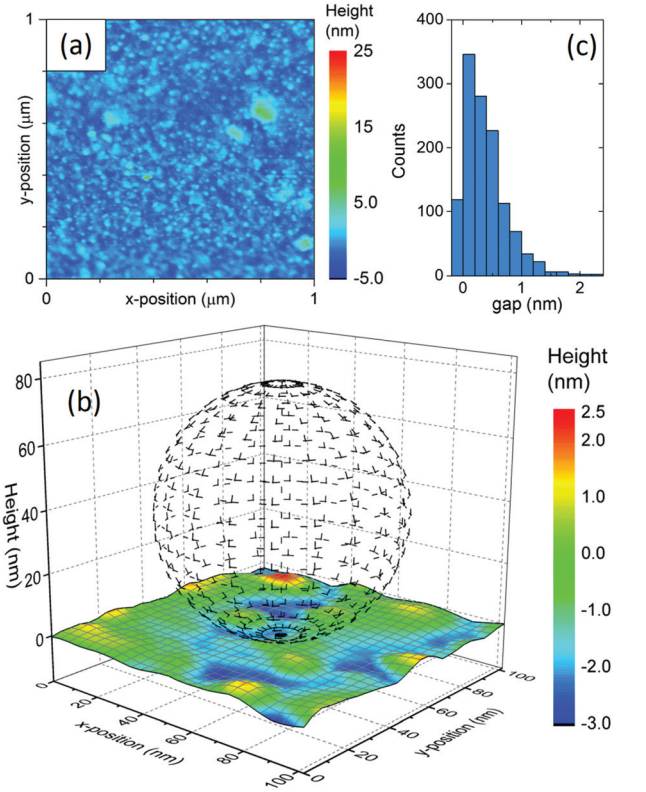

Fig. 2 (a) AFM image of a gold film thermally evaporated on glass. (b) Example surface geometry near a liquid-deposited gold nanoparticle deposited on top of the surface shown in (a). (c) Normalized gap size histogram from over 1200 possible particle locations.

the outline of an 80 nm diameter gold nanoparticle superimposed at the corresponding local *z*-minimum. Note that the measured local curvature of the gold film is similar to the known curvature of the gold nanosphere, implying that surface roughness can significantly affect the particle–substrate separation in the important junction region underneath the particle. Since the particle locations considered here represent local minima, the particle may have either one or three contact points with the substrate at these locations. In the case of one contact point the particle is separated from the metal film only by the thickness of the 4-MBT layer, while in the case of three contact points, an air gap may form directly underneath the particle. As will be shown below, the variation in this particle–substrate gap is a key factor in determining the variability in nanoparticle resonance spectra in substrate-tuned nanoparticle systems with finite surface roughness.

To determine whether gap size variation could account for the amount of spectral variation observed in the experiments, the geometrically predicted gap size was extracted for all possible particle positions obtained from the AFM data. Fig. 2(c) shows the gap size histogram obtained from analyzing over 1200 local particle height minima. The data is displayed at a bin size of 2 Å where the first bin extending from −2 Å to 0 Å represents particle positions that produce zero gap size (single contact point). A key point to note is that only 10% of the

particle locations produce zero gap size, suggesting that most deposited particles deposited randomly on this substrate will not have a contact point directly underneath the particle. While the obtained gaps and gap size variations are small, they can cause substantial variations in peak scattering wavelength.

To convert the gap sizes in Fig. 2(c) to predicted scattering spectra, representative geometries with a single contact point as well as geometries with three contact points and varying gap sizes were considered. The nanoscale local particle environment was modeled by defining three spherical protrusions on a gold film, arranged in an equilateral triangle and separated by a distance P as shown in Fig. 3(a). The gold film is assumed to be covered by a 0.5 nm thick layer of 4-MBT molecules, corresponding to the molecule used in the surface preparation.[12] Based on the known surface morphology from the AFM data the protrusions were chosen to have a radius of curvature (R_p) of $0.8R_{NP}$ and separation (P) of 25 nm respectively. This choice of P corresponds to the most prevalent spatial frequency present in the measured AFM scan of the gold surface, while the curvature of the protrusions is similar to typical surface curvature values throughout the AMF scan. Different air gap sizes (d) between the nanoparticle and the 4-MBT-coated gold film are achieved by varying the z-position of the protrusions. A side view of the resulting surface structure is shown in Fig. 3(b), corresponding to the plane marked by the vertical dashed line in Fig. 3(a). Note that the 0.5 nm thick molecular layer is too thin to be clearly visible in this sketch. Fig. 3(c) shows a perspective of one of the used geometries with an 80 nm diameter nanosphere superimposed.

The optical response of representative geometries was simulated using the method described in the Experimental section. Fig. 4(a) shows the simulated normalized scattering spectrum associated with the z-polarized dipole moment of a gold nanoparticle on a flat gold film. The spectrum shows a main z-polarized scattering peak at an energy of 1.59 eV (781 nm), somewhat lower than the typical spectral position of the main resonances in Fig. 1(b). A snapshot of the surface-normal field component is included for excitation at the peak wavelength as indicated by the arrow, revealing a gap plasmon resonance. Fig. 4(b) shows the corresponding results for a gold nanoparticle on a corrugated surface with d = 0 (dashed line). The corrugation is seen to cause a small red-shift of the main peak to 1.58 eV (786 nm) compared to the results in Fig. 4(a). The solid line shows the results for a corrugated structure with d = 0.39 nm, corresponding to the average gap size obtained from Fig. 2(c). The introduction of a 0.39 nm gap is seen to cause a significant blueshift of the main resonance peak to 1.71 eV (727 nm), close to the average resonance peak position of 1.67 eV in the experiment. Note that while the observed resonance shift relative to the free particle resonance wavelength of 580 nm is dominated by the coupling between the particle and the film, the refractive index of the molecular layer can contribute tens of nm to the total shift, depending on gap size. A snapshot of the surface-normal field distribution at this gap size is included for the peak wavelength as indicated by the arrow. The simulated scattering spectra at zero gap show clear secondary peaks at higher energy, which based on field snapshots (not shown) are attributed to higher order gap modes. Evidence for such modes appears to be present in several of the experimental spectra in

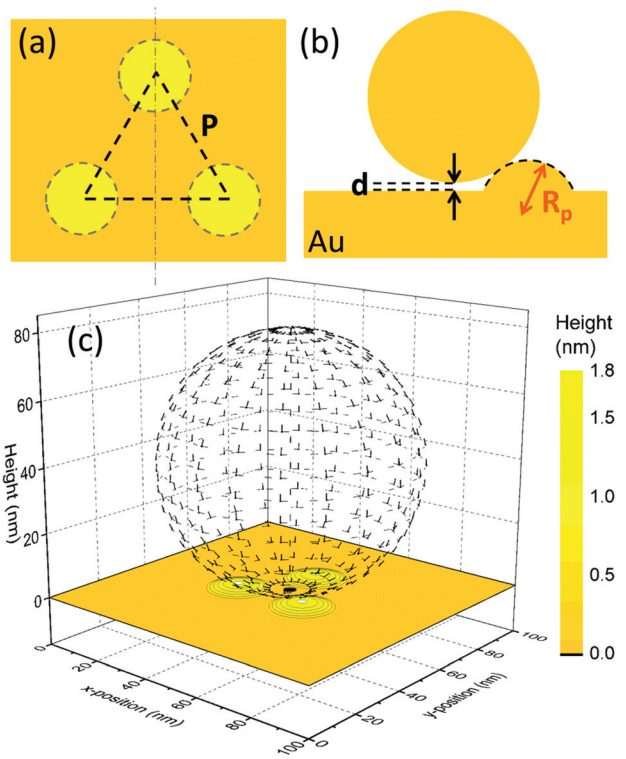

Fig. 3 Schematic of a representative simulation geometry and relevant parameters showing (a) a top view without a gold nanoparticle showing three protrusions, (b) a side view along the dashed line in (a) with a deposited gold nanoparticle present, and (c) a perspective view of the final structure.

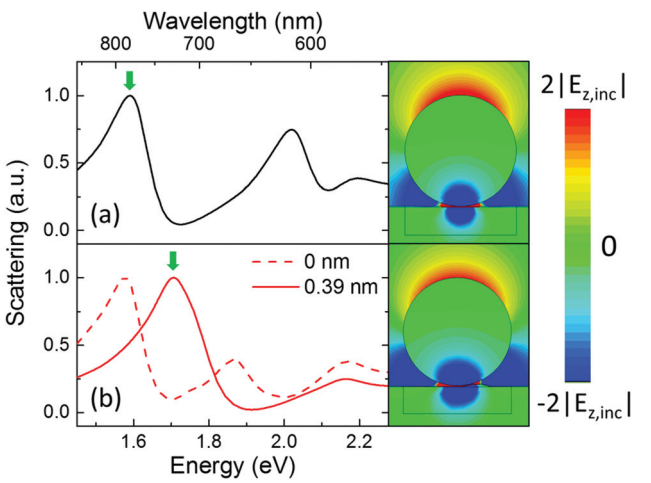

Fig. 4 Normalized scattering spectra of a gold nanoparticle (a) on a 4-MBT coated flat gold film and (b) on a corrugated gold surface with d = 0 (dashed line) and d = 0.39 nm (solid line). The field-plots show two-dimensional electric field distributions at the main resonance peak of the spectra as indicated by the green arrows.

Fig. 1(b), and intriguingly they indeed appear most prevalent in spectra with low-frequency main peaks. Based on the results presented in Fig. 4 it is clear that realistic changes in local surface geometry can produce spectral variations of a magnitude similar to those observed experimentally.

While the presented simulations demonstrate that roughness-related gap-size variations can account for the observed spectral fluctuations, the known particle size distribution in the used colloidal nanoparticle solution could also play a role. To investigate this possibility, particle-size dependent scattering spectra were calculated. Fig. 5(a) shows a contour graph of the simulated scattering spectra of gold nanoparticles with a diameter in the range 73.76 nm to 86.24 nm, deposited on a flat gold surface. This range matches the known 2σ particle size variation from the experiment. The main resonance energy of each simulated spectrum is marked by a black square for clarity. For comparison the horizontal black dashed line indicates the average resonance energy obtained from the measured scattering data, and the gray dashed lines correspond to the experimentally determined $\pm 2\sigma$ variation. The black solid line represents a linear fit to the simulated peak positions. All spectra show a strong low-frequency peak with a small redshift compared with the experimentally observed resonance wavelength as well as a short wavelength peak previously attributed to a higher order gap resonance. As the particle size is increased, a small redshift of the main resonance is observed. Based on the known size variation and the size-dependent simulated scattering spectra, an average resonance energy of 1.59 eV and a 2σ spectral variation of ±17.5 meV are predicted, as indicated by the blue circle and its energy error bars. These values are notably smaller than the spectral variation observed in the experiments, demonstrating that particle size variation alone is not sufficient to explain the experimental results.

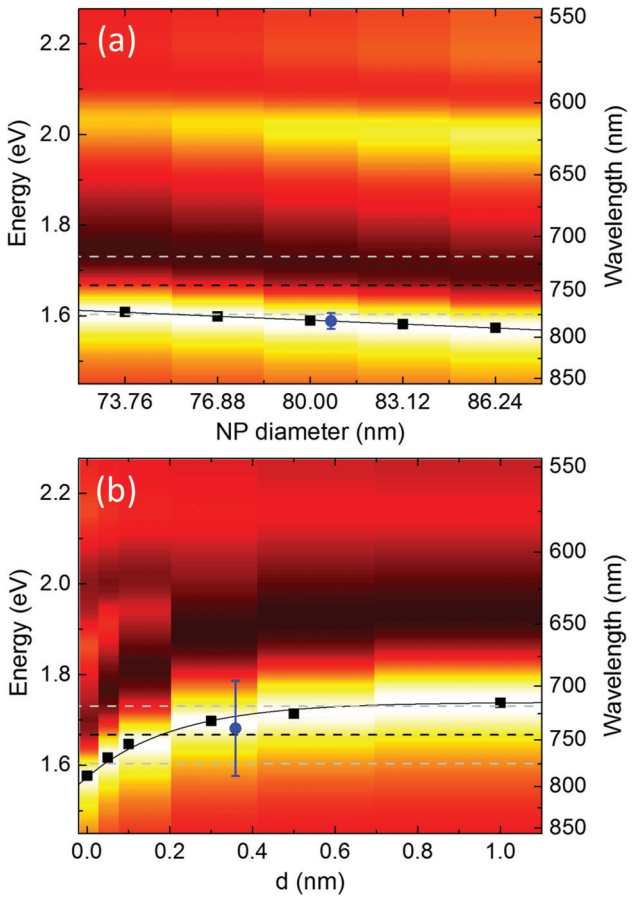

Fig. 5 (a) Contour graph of the scattering spectra of gold nanoparticles with different sizes on a flat gold film. (b) Contour graph of the scattering spectra of an 80 nm diameter gold nanoparticle on a rough surface as a function of air gap size d. The black dashed line represents the average resonance energy from the experiment and the two grey dashed lines span 2σ on each side. The black squares mark the main peak positions and the solid lines show empirical fits to the peak position. The blue circles represent experimentally expected spectral positions and variations based on numerical simulations.

To quantitatively compare the measured and predicted spectral variations related to surface roughness effects, simulations of the rough surface with different gap sizes were carried out. Fig. 5(b) shows a contour graph of the scattering spectra of 80 nm diameter gold nanoparticles on a rough surface with $R_p = 0.8R_{NP}$ and $P = 25$ nm as a function of gap size. The black solid line represents an empirical fit to the data. As the gap size is increased the low-energy peak in the scattering spectra blueshifts from 1.58 eV to 1.74 eV. This simulated gap-size-dependence of the main scattering peak was used to convert the gap size histogram (Fig. 2(b)) to a resonance energy histogram. The thus obtained average resonance energy of 1.68 eV is shown as a blue circle in Fig. 5(b) while the error bar of ±105 meV shows the predicted 2σ variation. The predicted resonance energy and variation agree reasonably well with those of the measured spectra which show an average resonance at 1.67 eV and 2σ = 63 meV. It should be pointed out that the observed spectral variation of substrate-tuned nanoparticle plasmon resonances could be improved by using alternate substrate preparation techniques that minimize surface roughness, including template stripping[13] or the use of chemically synthesized single-crystal gold films.[14] A final point worth noting is that the analysis presented here does not consider the nanoparticle-mediated excitation of propagating surface plasmon polaritons (SPPs). While the gold nanoparticles are expected to allow for such coupling, this effect is not expected to strongly affect to the gap plasmon resonance energy due to the large mode size mismatch between the gap mode (typical size tens of nm) and SPPs at these wavelengths (lateral extent of tens of μm) resulting in relatively weak SPP excitation.

The numerical simulations demonstrate that a typical roughness as small as ~1 nm on a thermally evaporated gold film is sufficient to significantly affect the gap plasmon resonance of 80 nm diameter particles. This is a consequence of the fact that gap plasmon modes of supported nanoparticles become strongly confined at small particle–substrate separations, making the resonances extremely sensitive to the exact nanoscale geometry near the particle–substrate junction. The effect of local geometry is expected to be slightly less pronounced

when taking into account nonlocal effects, which are known to lead to a blueshift in the gap resonance frequency and a weaker dependence of resonance wavelength on small gap sizes.[15]

Conclusions

We have investigated the effect of surface roughness on the gap plasmon resonance of gold nanoparticles on a thermally evaporated gold film. The measured single particle scattering spectra show spectral variation that can be attributed to random variations in the local environment of the gold nanoparticles due to nanoscale surface roughness. The magnitude of the observed spectral variation is reproduced in numerical simulations of a gold nanoparticle on gold films with realistic roughness. The approach presented here could be used to predict spectral performance of any nanoparticle-on-film based plasmonic platform with known roughness, without the need to map the exact local surface morphology of each individual particle.

Experimental

Sample preparation

Sample preparation involved the thermal evaporation of a 2 nm thick chromium wetting layer onto a glass cover slip (Thermo scientific) immediately followed by the thermal evaporation of a gold film. The resulting gold film thickness was measured using variable angle spectroscopic ellipsometry, and was found to be 48.7 ± 0.5 nm. The root mean square film roughness of the film was found to be ~1 nm as measured using tapping-mode atomic force microscopy (AFM). The substrate was then incubated in a 10^{-3} mol L^{-1} 4-methylbenzenethiol (Sigma Aldrich) solution in ethanol for two hours. Subsequently the substrate was thoroughly rinsed with ethanol and dried using compressed air. This procedure produces a self-assembled monolayer of 4-MBT molecules on a gold film,[12,16,17] representative of a typical Surface Enhanced Raman Scattering (SERS) test structure. Gold nanoparticles were deposited onto the substrate by incubating the substrate for 10 minutes in an 80 nm gold nanoparticle solution (BBInternational, batch-specific mean diameter of 80.7 nm with size variation $2\sigma < 7.8\%$) diluted in ethanol to a concentration of 5×10^8 particles mL^{-1}. The substrate was subsequently rinsed with ethanol and dried using compressed air. The method resulted in a low particle areal density enabling single particle spectroscopy.

Optical microscopy and spectroscopy

Optical microscopy and single particle spectroscopy of gold nanoparticles on the gold films were carried out using an inverted microscope (Olympus IX71). A Canon EOS 450D digital camera was used for image capture, and an imaging spectrometer attached to the microscope (Horiba iHR320 with Synapse CCD array) was used for single particle spectroscopy. Scattering spectra were obtained using a 50× dark field objective with an illumination angle of ~77° (Olympus UMPlanFl 50× BD, N.A. = 0.75). The scattered light from the particle was collected by the same objective and sent to either the camera or the spectrometer. For spectroscopy, the collection area was set to be 6 μm × 2.6 μm by limiting the spectrometer entrance slit width and using vertical binning of the recorded CCD data. The spectral resolution in all measurements was 6 nm. Single-particle scattering spectra I_{sc} were obtained by using the relation $I_{sc} = (S - R)/R$, where S and R were the collected signal from an area containing a nanoparticle and a nearby region without nanoparticles, respectively. The subtraction removes any background signal related to scattering from the substrate. The obtained scattering spectra were peak-normalized to facilitate comparison.

Simulation

The optical response of representative geometries was simulated using the three-dimensional frequency domain finite integration technique,[18] following the method described in ref. 5. Briefly, a simulation volume of 240 × 240 × 310 nm^3 was illuminated with a p-polarized electromagnetic wave at an angle of incidence of 77°, corresponding to the illumination angle used in the experiment, and the scattering spectrum is obtained from the dipole moment of the nanoparticle. The dielectric function of gold was taken from the literature[19] and the refractive index of the molecular layer was assumed to be 1.55. The laterally polarized dipole component which is responsible for the green scattering spot was not considered in this calculation due to its small contribution to the main resonance peak.[5,6,20,21]

Acknowledgements

This work has been made possible thanks to the financial support from the National Science Foundation (NSF CHE-1213182). Support for Dr. Binfeng Yun was provided by the China State Scholarship Foundation (No. 2010832300). The authors would like to thank Hemma Mistry, Mahdi Ahmadi, and Prof. Beatriz Roldan Cuenya for the Atomic Force Microscopy measurements used in this work.

Notes and references

1 J. J. Mock, R. T. Hill, Y. J. Tsai, A. Chilkoti and D. R. Smith, *Nano Lett.*, 2012, **12**, 1757–1764.
2 D. Y. Lei, A. I. Fernandez-Dominguez, Y. Sonnefraud, K. Appavoo, R. F. Haglund, J. B. Pendry and S. A. Maier, *ACS Nano*, 2012, **6**, 1380–1386.
3 S. Mubeen, S. P. Zhang, N. Kim, S. Lee, S. Kramer, H. X. Xu and M. Moskovits, *Nano Lett.*, 2012, **12**, 2088–2094.
4 L. Li, T. Hutter, U. Steiner and S. Mahajan, *Analyst*, 2013, **138**, 4574–4578.

5 C. Lumdee, S. Toroghi and P. G. Kik, *ACS Nano*, 2012, **6**, 6301–6307.
6 C. Lumdee, B. Yun and P. G. Kik, *J. Phys. Chem. C*, 2013, **117**, 19127–19133.
7 S. Link and M. A. El-Sayed, *J. Phys. Chem. B*, 1999, **103**, 4212–4217.
8 K. S. Lee and M. A. El-Sayed, *J. Phys. Chem. B*, 2006, **110**, 19220–19225.
9 J. J. Mock, M. Barbic, D. R. Smith, D. A. Schultz and S. Schultz, *J. Chem. Phys.*, 2002, **116**, 6755–6759.
10 P. A. Kossyrev, A. J. Yin, S. G. Cloutier, D. A. Cardimona, D. H. Huang, P. M. Alsing and J. M. Xu, *Nano Lett.*, 2005, **5**, 1978–1981.
11 G. Hajisalem, Q. Min, R. Gelfand and R. Gordon, *Opt. Express*, 2014, **22**, 9604–9610.
12 G. Sauer, G. Brehm and S. Schneider, *J. Raman Spectrosc.*, 2004, **35**, 568–576.
13 M. Hegner, P. Wagner and G. Semenza, *Surf. Sci.*, 1993, **291**, 39–46.
14 J. S. Huang, V. Callegari, P. Geisler, C. Bruning, J. Kern, J. C. Prangsma, X. F. Wu, T. Feichtner, J. Ziegler, P. Weinmann, M. Kamp, A. Forchel, P. Biagioni, U. Sennhauser and B. Hecht, *Nat. Commun.*, 2010, 1.
15 C. Ciraci, R. T. Hill, J. J. Mock, Y. Urzhumov, A. I. Fernandez-Dominguez, S. A. Maier, J. B. Pendry, A. Chilkoti and D. R. Smith, *Science*, 2012, **337**, 1072–1074.
16 M. A. Khan, T. P. Hogan and B. Shanker, *J. Raman Spectrosc.*, 2008, **39**, 893–900.
17 A. Ulman, *Chem. Rev.*, 1996, **96**, 1533–1554.
18 CST MICROWAVE STUDIO®, *Computer Simulation Technology*, Darmstadt, Germany, 2013.
19 P. B. Johnson and R. W. Christy, *Phys. Rev. B: Solid State*, 1972, **6**, 4370–4379.
20 R. T. Hill, J. J. Mock, Y. Urzhumov, D. S. Sebba, S. J. Oldenburg, S. Y. Chen, A. A. Lazarides, A. Chilkoti and D. R. Smith, *Nano Lett.*, 2010, **10**, 4150–4154.
21 S. Y. Chen, J. J. Mock, R. T. Hill, A. Chilkoti, D. R. Smith and A. A. Lazarides, *ACS Nano*, 2010, **4**, 6535–6546.